Signal-coupled subthreshold Hopf-type systems show a sharpened collective response

Gomez, Florian ; Lorimer, Tom ; Stoop, Ruedi

Abstract: Astounding properties of biological sensors can often be mapped onto a dynamical system below the occurrence of a bifurcation. For mammalian hearing, a Hopf bifurcation description has been shown to work across a whole range of scales, from individual hair bundles to whole regions of the cochlea. We reveal here the origin of this scale invariance, from a general level, applicable to all dynamics in the vicinity of a Hopf bifurcation (embracing, e.g., neuronal Hodgkin-Huxley equations). When subject to natural "signal coupling," ensembles of Hopf systems below the bifurcation threshold exhibit a collective Hopf bifurcation. This collective Hopf bifurcation occurs at parameter values substantially below where the average of the individual systems would bifurcate, with a frequency profile that is sharpened if compared to the individual systems.

DOI: https://doi.org/10.1103/PhysRevLett.116.108101

Signal-Coupled Subthreshold Hopf-Type Systems Show a Sharpened Collective Response

Florian Gomez, Tom Lorimer, and Ruedi Stoop*
Institute of Neuroinformatics and Institute of Computational Science, University of Zurich and ETH Zurich, 8057 Zurich, Switzerland
(Received 27 August 2015; published 9 March 2016)

Astounding properties of biological sensors can often be mapped onto a dynamical system below the occurrence of a bifurcation. For mammalian hearing, a Hopf bifurcation description has been shown to work across a whole range of scales, from individual hair bundles to whole regions of the cochlea. We reveal here the origin of this scale invariance, from a general level, applicable to all dynamics in the vicinity of a Hopf bifurcation (embracing, e.g., neuronal Hodgkin-Huxley equations). When subject to natural "signal coupling," ensembles of Hopf systems below the bifurcation threshold exhibit a collective Hopf bifurcation. This collective Hopf bifurcation occurs at parameter values substantially below where the average of the individual systems would bifurcate, with a frequency profile that is sharpened if compared to the individual systems.

DOI: 10.1103/PhysRevLett.116.108101

Biological sensors often deal with inputs across many orders of magnitude (expressed by a logarithmic stimulus scale, e.g., decibel or pH scales). They usually have the ability to strongly amplify weak inputs and to compress higher input levels. Prominent manifestations are the hearing system with its "compressive nonlinearity" [1,2] and the nonlinear input or frequency response of neurons. Such properties emerge naturally from dynamical systems below a bifurcation point (a bifurcation is a mathematical term describing a structural change of a solution of a dynamical system). This was already known 30 years ago, then termed "small-signal amplification" [3–5]. Its important role as the working principle of biological sensors was recognized much later [6,7]; in particular, the mechanism was shown to play a decisive role in insect hearing [8,9]. Regarding mammalian hearing [1,10–12], this principle still is fighting its way against classical engineering hearing solutions. For networks of neurons, which naturally display bifurcation behavior, the corresponding consequences have largely remained unexplored. Here, we demonstrate novel phenomena of collective behavior of potential biological significance that emerge from this phenomenon. To date, investigations of models of biological neuronal networks have mostly focused on the synchronization of pulse-coupled phase oscillators [13–15] or integrate and fire neurons [16–18], which generally do not incorporate a Hopf bifurcation regime.

For the subthreshold Hopf bifurcation regime that we focus on here, only singular exemplary studies in the context of the Hopf cochlea have been conducted (notably Ref. [12]); a more general study comparable to the super-threshold (i.e., self-oscillatory) case is still missing. In nature, different types of bifurcations occur that mathematics classifies according to the eigenvalues that the system's linearization has when the behavioral change occurs, i.e., at the bifurcation point. The Hopf bifurcation is among the most fundamental bifurcations in physics and biology [1,6,10,11,19]. In addition to the small-signal amplifier properties, it has a sharp tuning regarding stimulation frequency (a feature shared by some other, more specific, bifurcations). "Hopf systems" (for short) are at rest below the bifurcation point. When pushed by a stimulus, this signal is amplified more (i) the closer the system is to its bifurcation point; (ii) the closer the signal's frequency content is to the system's preferred frequency; and (iii) the smaller the input's amplitude [Figs. 1(a) and 1(b)]. If, due to a suitable external parameter change, a Hopf system crosses the bifurcation point, it starts to oscillate (or "spike") in a self-sustained manner, at a system-characteristic frequency.

In the cochlea, single outer hair cells as well as mesoscopic cochlea elements of hundreds of hair cells [10,20] are reliably described by a Hopf system. In this Letter, we elucidate how a single element and ensembles composed of these elements adhere to the same physical description, and what this entrains further. We will show that, when coupled by means of their output signals, an ensemble of subthreshold Hopf systems has the collective behavior of a small-signal amplifier. When the coupling is sufficiently strong, the ensemble may undergo a Hopf bifurcation, where the systems spontaneously oscillate in a synchronized manner. In both regimes, the behavior of the ensemble is indistinguishable from that of a single Hopf system. In the subthreshold regime, the regime that we are interested in, this happens with a significantly sharpened frequency response profile and a much increased input sensitivity, if compared to the contributing systems [Fig. 1(a) vs 1(d)]. Such behavior is fundamentally different from the bulk of studies focusing on coupled oscillators (e.g., [21–23]).

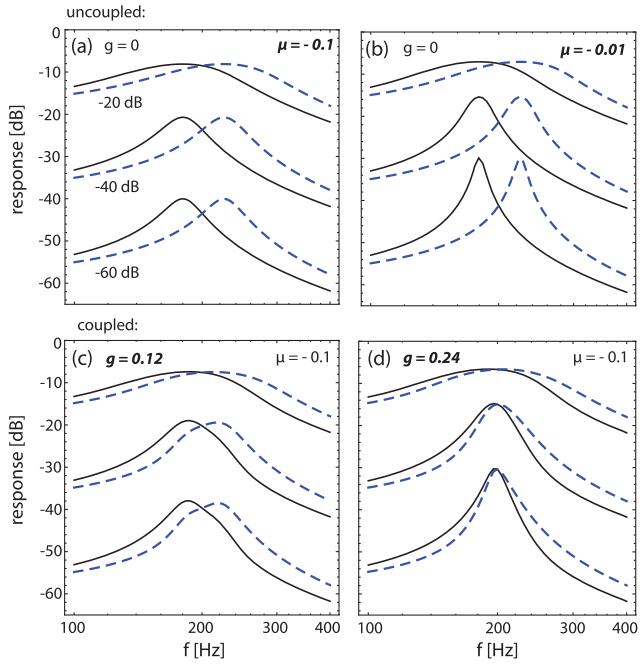

FIG. 1. Response of two Hopf systems in Eq. (2) with characteristic frequencies $\omega_{1,2}/2\pi = 180$ and 225 Hz (solid and dashed curves, respectively) to a periodic test signal with variable frequency $f = \omega/2\pi$ at three amplitudes −20, −40, and −60 dB. Uncoupled systems ($g = 0$): (a) and (b). Coupled systems: (c) $g = 0.12$ and (d) $g = 0.24$.

To demonstrate these claims, we start from the frequency-rescaled unforced Hopf equation

$$\dot{z} = (\mu + i)\omega_{\mathrm{ch}} z - \omega_{\mathrm{ch}}|z|^2 z, \tag{1}$$

where $z(t)$ is the complex-valued variable, μ is the distance to the bifurcation point, and ω_{ch} is the characteristic (angular) frequency of the system [20]. In this formulation, a Hopf bifurcation occurs when the parameter μ changes from negative to positive values: For $\mu > 0$, the system starts to spontaneously oscillate at a frequency ω_{ch}. Below bifurcation (i.e., for $\mu < 0$), the system is quiet, but a periodic stimulation signal of angular frequency ω is amplified, more strongly the closer ω is to ω_{ch} and the closer the system is to bifurcation. Allowing two such Hopf systems to interact via their output signals, i.e., by *signal coupling*, yields

$$\begin{aligned} \dot{z_1} &= \omega_1\left[(\mu_1 + i)z_1 - |z_1|^2 z_1 + \frac{g_{21}}{2} z_2\right], \\ \dot{z_2} &= \omega_2\left[(\mu_2 + i)z_2 - |z_2|^2 z_2 + \frac{g_{12}}{2} z_1\right], \end{aligned} \tag{2}$$

where $\omega_{1,2}$ are the characteristic frequencies of the systems and g_{ij} denotes the coupling from system i to system j. This situation will be generalized; the factor of $1/2$ is introduced to facilitate the generalization to N systems later on. We emphasize that such a setting is different from diffusive coupling and has previously, in the context of laser systems, also been referred to as "injective" coupling [24]. Diffusive coupling is by convention coupling via a term proportional to the state difference between the coupled nodes, that is additive to the individual node dynamics; see, e.g., [24–30]. Two settings that are based on, in some sense, similar couplings to what we consider here were previously investigated in the superthreshold regime: A first example demonstrated complex behavior as a function of the system parameters, in particular, regarding amplitude death [29], whereas a second example exhibited the crucial role of the coupling for the synchronization between self-sustained circadian oscillator neurons in the suprachiasmatic nucleus of mammals [31].

How then does signal coupling affect the subthreshold behavior of Hopf systems? To measure the small-signal amplification, we add for each system to the right-hand side of Eq. (1) a test signal

$$h(t) = \omega_{\mathrm{ch}} h_0 e^{i\omega t}$$

and measure the responses for different values of g and ω. The form of the test signal incorporates that input arriving at the node will be scaled by a node's characteristic frequency, distinguishing in this way between more and less excitable systems. For $\omega_1/2\pi = 180$ Hz, $\omega_2/2\pi = 225$ Hz, and $\mu = -0.1$, the result is displayed in Figs. 1(c) and 1(d), compared to the uncoupled case (a) and (b), respectively. From this, the evident effect of signal coupling is a transition from two individual, rather broad, response profiles to two almost overlapping sharply peaked profiles at $g = 0.24$. The pronounced small-signal amplification characteristics around the center frequency $f_c = 200$ Hz can be seen as an indication that the signal-coupled system might be in the vicinity of a Hopf bifurcation. To investigate the role of the coupling g, we keep the Hopf parameter $\mu_1 = \mu_2 = \mu$ fixed and find that, at a "critical coupling" g_c, the origin $z_1 = z_2 = 0$ loses stability; beyond g_c, the ensemble of the two systems starts to oscillate spontaneously at a frequency f_c. Close to bifurcation (here, $g_c \approx 0.3$), the response curves are comparable to those of an individual system at $\mu \simeq -0.01$ [see Fig. 1(b)] but display a frequency response sharply tuned around a common center frequency.

To prove that the coupled system is of the Hopf type, we first analyze the system's behavior at an equal distance below bifurcation $\mu_1 = \mu_2 = \mu < 0$, for variable symmetric coupling strength $g = g_{12} = g_{21}$ and variable characteristic frequencies. We will see that this system has improved small-signal properties, compared to the individual contributing systems. While the proof can be extended to cover the case of a larger number of Hopf systems having individually variable Hopf parameters and couplings, in this Letter, we will present only the numerical corroboration. To investigate the properties at critical coupling g_c in

dependence of $\omega_{1,2}$ and μ, we rewrite the system as a four-dimensional real-valued system. We find for the origin fixed point solution the Jacobian

$$J = \begin{pmatrix} \mu\omega_1 & -\omega_1 & \frac{g}{2}\omega_1 & 0 \\ \omega_1 & \mu\omega_1 & 0 & \frac{g}{2}\omega_1 \\ \frac{g}{2}\omega_2 & 0 & \mu\omega_2 & -\omega_2 \\ 0 & \frac{g}{2}\omega_2 & \omega_2 & \mu\omega_2 \end{pmatrix}. \quad (3)$$

The stability is determined by the real part Re of the eigenvalues of the Jacobian. At the Hopf bifurcation, two complex conjugate eigenvalues cross the imaginary axis, which can be used to determine the critical coupling value g_c. After some simplifications, we arrive at the implicit equation

$$(\omega_1+\omega_2)\mu = -\mathrm{Re}\left(\sqrt{(\mu^2-1+2\mu i)(\omega_1^2-\omega_2^2)+g_c^2\omega_1\omega_2}\right). \quad (4)$$

Solving this equation numerically for g_c yields a function $g_c(\omega_2/\omega_1, \mu)$. The obtained results (Fig. 2) express that coupling strongly enhances the emergence of a (collective) oscillation. If the two systems have identical characteristic frequencies $\omega_1 = \omega_2$, we obtain from Eq. (4) $g_c = -2\mu$, which determines the location of the minima of the curves. Pushing either system frequency into one direction increases g_c. Similarly, pushing μ further away from the bifurcation point $\mu = 0$ shifts g_c to higher values. Conversely, for all couplings g, we may cross the bifurcation point by changing μ. In this sense, μ does not fully abandon its role as a bifurcation parameter. However, the critical value is no longer $\mu_c = 0$ of the uncoupled systems but shifts to more negative values, expressing that the coupled system is more excitable than its components. For symmetric coupling, the center frequency f_c also provides the frequency of the oscillation after bifurcation. f_c also coincides with the stimulus frequency to which the individual uncoupled systems would respond with equal strength. A simple calculation yields its value as

$$\omega_c = 2\pi f_c = \frac{2\omega_1\omega_2}{\omega_1+\omega_2}. \quad (5)$$

For the example provided above ($\omega_1/2\pi = 180$ Hz and $\omega_2/2\pi = 225$ Hz, $\mu = -0.1$), we indeed obtain $f_c = 200$ Hz (cf. Fig. 1). Above the bifurcation, the system maintains f_c as long as $g_{12} = g_{21}$.

For asymmetrical coupling, g_c^2 in Eq. (4) has to be replaced by $g_{12}g_{21}$. For, e.g., g_{12} fixed, we easily find the critical value of g_{21} (cf. Fig. 3, where in the g_{12}-g_{21} space the numerically obtained critical line, together with the oscillation frequency after the bifurcation, is displayed). For asymmetrical coupling, the oscillation frequency shifts towards the dominant system's characteristic frequency (cf. Fig. 3). For completeness, we note that diffusive coupling of our subthreshold Hopf systems would *stabilize* the system instead of making it more excitable: To arrive at collective self-oscillations, the individual bifurcation values would have to be augmented to significantly positive values (typically $\mu > 0.1$).

After having secured that the coupling maintains the Hopf property, we investigate how an ensemble's Hopf bifurcation point depends on the ensemble size N. For our numerical

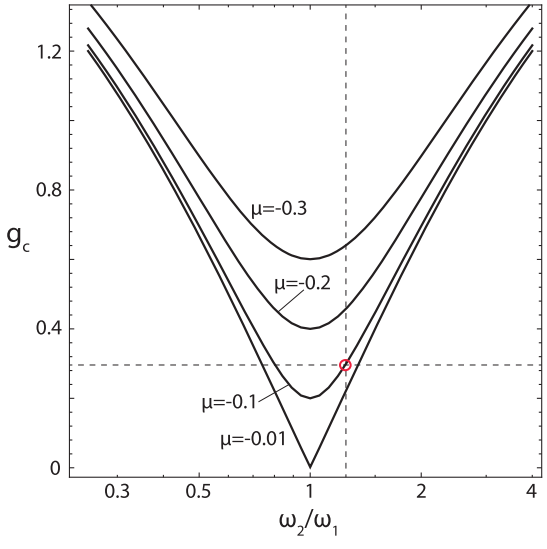

FIG. 2. Critical value g_c for symmetric coupling $g = (g_{12} = g_{21})$, as a function of ω_2/ω_1, where $\omega_1/2\pi = 180$ Hz, for four values of μ. The lines single out the regions above which the coupled system starts to oscillate, based on elements that are individually below the bifurcation threshold. Red circle: Location of g_c for $\omega_1/2\pi = 180$ and $\omega_2/2\pi = 225$ Hz.

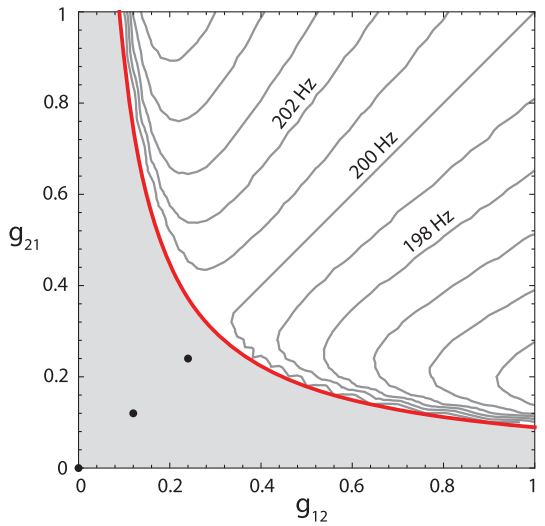

FIG. 3. Critical coupling g_c (red line) and frequency of oscillation (contours) above the bifurcation for asymmetrical coupling ($\omega_{1,2}/2\pi = 180$ and 225 Hz, $\mu_{1,2} = -0.1$). Gray-shaded area: Small-signal amplification regime. Black dots: Location of the systems of Figs. 1(a), 1(c), and 1(d).

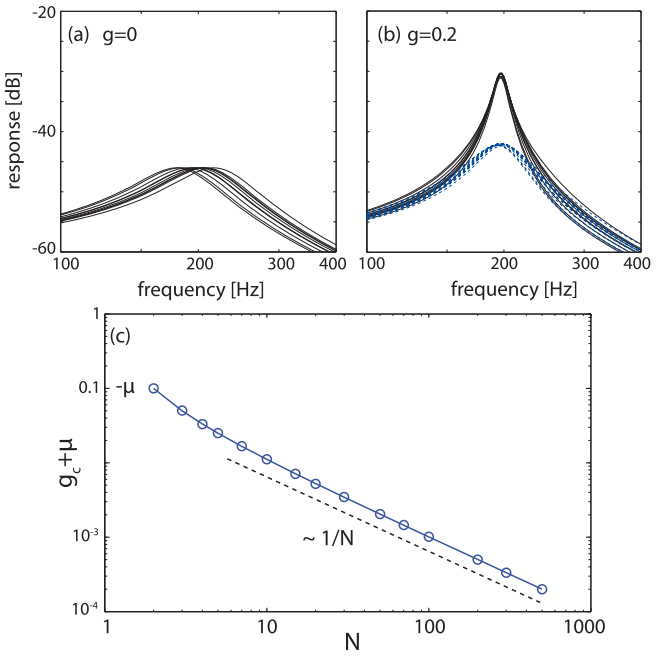

FIG. 4. Response of $N = 10$ systems, characteristic frequencies distributed around 200 Hz, to a test signal of amplitude −60 dB. (a) Uncoupled, $\mu = -0.2$, (b) signal-coupled (dashed curve, $\mu = -0.3$; solid curve, $\mu = -0.2$), exhibiting a coherent and sharply tuned response around $f_c \approx 200$ Hz. (c) $g_c + \mu$ as a function of N, for $\omega_{\mathrm{ch},i} = \omega_{\mathrm{ch}}$ and $\mu_i = \mu = -0.1$. The same behavior (with a line shift) is obtained for reasonable variations of $\omega_{\mathrm{ch},i}$ and μ_i. The value of μ is reflected in the first data point obtained for $N = 2$, which implies $g_c = -2\mu$ [cf. Eq. (5) and Fig. 2].

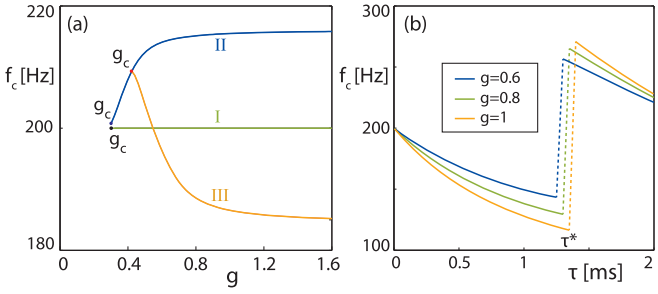

FIG. 5. (a) f_c as a function of the coupling g beyond g_c ($\mu = -0.1$ for all systems). (I) Two systems (180/225 Hz); (II) three systems (180, 200, and 300 Hz); (III) five systems (120, 160, 200, 240, and 300 Hz). (b) f_c for τ-delayed coupling (two systems at 180 and 225 Hz, $\mu_{1,2} = -0.1$).

experiments, we used the all-to-all topology (replacing $g/2$ by g/N); other coupling topologies yield qualitatively similar effects. Our results shown in Figs. 4(a) and 4(b) corroborate for an ensemble of $N = 10$ systems, with frequencies distributed around 200 Hz, the expected small-signal amplification characteristics of a single Hopf system, at augmented excitability, with a simple scaling relation of exponent −1 [Fig. 4(c)]. Without requiring a precise building principle, signal coupling drives the ensemble towards a common characteristic frequency f_c and establishes a coherent response profile that is largely independent of the individual system frequency distribution.

The strength of our setting becomes apparent when identifying it as a paradigm of coupled auditory hair cells. While Refs. [32–36] used very detailed hair-cell models (involving a multitude of equations and parameters), we obtain what we see as the most salient results [34] by coupling subthreshold normal-form Hopf systems [cf. Fig. 4(c)]. By relaxing all-to-all to local coupling, we observed the emergence of synchronized subnetworks similar to the superparamagnetic phase in statistical physics, a paradigm that has been proven to be computationally extremely efficient, e.g., for clustering [37]. We expect such approaches to become pivotal for getting a grip on the claimed increased computational efficacy of deep layer neural networks [38], for understanding of the behavior and function of the mammalian suprachiasmatic nucleus [31,39–41], or for the explanation of the emergence of spontaneous otoacoustic emissions [42,43] in the cochlea.

How well does our paradigm reflect also the behavior of (synchronized) neurons in the *superthreshold* regime? Beyond the bifurcation, our center frequency f_c becomes a more complicated function of the coupling g [Fig. 5(a)]. While for two systems f_c remains fixed (I), for more systems, $f_c(g)$ can either increase (II) or decrease (III) with g, until saturation dominates. Introducing a time delay τ into the coupling, where, for two systems, the couplings in Eqs. (2) would be replaced by $\frac{g_{21}}{2} z_2(t-\tau)$ and $\frac{g_{12}}{2} z_1(t-\tau)$, maintains a nontrivial dependence of f_c on the coupling but introduces an even richer behavior. For N systems, we considered that each system obtains from all other systems the same time-delayed signal. This is a simple setting, in particular, from the cochlear perspective, but is sufficient to assess the general effect of a signal delay. For small delays ($\tau < 1$ ms), even for two systems f_c changes with the coupling strength and delay [Fig. 5(b)], where the dependence has some resemblance to that of coupled limit-cycle systems [44]; for a similar behavior in suprachiasmatic nucleus modeling, see Ref. [45]. At larger delays $\tau^*(g)$, a discontinuous jump of f_c occurs. This is repeated upon further increased delays, a phenomenon that parallels the change of locking observed in driven systems. The critical coupling value g_c varies with τ only mildly, in contrast to the behavior shown by f_c.

Also for coupled realistic neurons, the synchronization frequency is a function of the coupling strength; this is in full contrast to the *invariable* synchronization frequency of diffusively coupled Kuramoto phase oscillators [46]. In our paradigm, f_c depends primarily on the distribution of the system frequencies ω_i. A bias in the coupling changes the relative dominance among the systems and introduces a change in f_c. Only for perfectly symmetrical situations (e.g., 180, 200, and 225 Hz or 100, 100, 200, and 200 Hz) do we have $f_c = \mathrm{const}$. In many biology-relevant cases, a

paradigm that exhibits such a coupling-dependent frequency might be more appropriate than the abstract equilibrium-motivated diffusive coupling. More generally, Hopf systems are prototypes of biological excitability [19,47–49]. Upon an appropriate input from other nodes, often strongly dependent on external sources, such elements are activated, a property that is shared by most biological neurons. The presently dominant modeling of neuronal ensembles by diffusively coupled Kuramoto phase oscillators [50–52] misses this aspect. Models with flexible bifurcation parameters, as used here, may lead to a more thorough understanding of how information is processed in biological networks.

This work was supported by the Swiss National Science Foundation (Grant No. 200020-147010/1 and Grant No. 200021-153542/1 to R. S.).

*Corresponding author.
ruedi@ini.phys.ethz.ch

[1] A. J. Hudspeth, Neuron **59**, 530 (2008).
[2] J. Ashmore *et al.*, Hear. Res. **266**, 1 (2010).
[3] K. Wiesenfeld and B. McNamara, Phys. Rev. Lett. **55**, 13 (1985).
[4] K. Wiesenfeld and B. McNamara, Phys. Rev. A **33**, 629 (1986).
[5] B. Derighetti, M. Ravani, R. Stoop, P. F. Meier, E. Brun, and R. Badii, Phys. Rev. Lett. **55**, 1746 (1985).
[6] V. M. Eguíluz, M. Ospeck, Y. Choe, A. J. Hudspeth, and M. O. Magnasco, Phys. Rev. Lett. **84**, 5232 (2000).
[7] S. Camalet, T. Duke, F. Jülicher, and J. Prost, Proc. Natl. Acad. Sci. U.S.A. **97**, 3183 (2000).
[8] R. Stoop, A. Kern, M. C. Göpfert, D. A. Smirnov, T. V. Dikanev, and B. P. Bezrucko, Eur. Biophys. J. **35**, 511 (2006).
[9] T. Lorimer, F. Gomez, and R. Stoop, Sci. Rep. **5**, 12492 (2015).
[10] A. Kern and R. Stoop, Phys. Rev. Lett. **91**, 128101 (2003).
[11] M. O. Magnasco, Phys. Rev. Lett. **90**, 058101 (2003).
[12] M. Golubitzky, L. Shiau, C. Postlethwaite, and Y. Zhang, in *Coherent Behavior in Neuronal Networks*, edited by K. Josic, R. Rubin, and M. Matias, Springer Series in Computational Neuroscience Vol. 3 (Springer, Heidelberg, 2009).
[13] J. G. Restrepo, E. Ott, and B. R. Hunt, Chaos **16**, 015107 (2006).
[14] I. Sendiña-Nadal, J. M. Buldú, I. Leyva, and S. Boccaletti, PLoS One **3**, e2644 (2008).
[15] T. Girnyk, M. Hasler, and Y. Maistrenko, Chaos **22**, 013114 (2012).
[16] S. Luccioli and A. Politi, Phys. Rev. Lett. **105**, 158104 (2010).
[17] S. Olmi, A. Politi, and A. Torcini, Europhys. Lett. **92**, 60007 (2010).
[18] K. P. O'Keeffe, P. L. Krapivsky, and S. H. Strogatz, Phys. Rev. Lett. **115**, 064101 (2015).
[19] A. L. Hodgkin and A. F. Huxley, J. Physiol. **117**, 500 (1952).
[20] S. Martignoli, J.-J. van der Vyver, A. Kern, Y. Uwate, and R. Stoop, Appl. Phys. Lett. **91**, 064108 (2007).
[21] D. G. Aronson, G. B. Ermentrout, and N. Kopell, Physica D (Amsterdam) **41**, 403 (1990).
[22] S. H. Strogatz, Physica D (Amsterdam) **143**, 1 (2000).
[23] G. B. Ermentrout and D. Kleinfeld, Neuron **29**, 33 (2001).
[24] J. González-Miranda, *Synchronization and Control of Chaos: An Introduction for Scientists and Engineers* (Imperial College Press, London, 2004).
[25] H. Fujisaka and T. Yamada, Prog. Theor. Phys. **69**, 32 (1983).
[26] L. M. Pecora and T. L. Carroll, Phys. Rev. Lett. **80**, 2109 (1998).
[27] T. Pereira, J. Eldering, M. Rasmussen, and A. Veneziani, Nonlinearity **27**, 501 (2014).
[28] E. Rossoni, Y. Chen, M. Ding, and J. Feng, Phys. Rev. E **71**, 061904 (2005).
[29] W. Zou, D. V. Senthilkumar, R. Nagao, I. Z. Kiss, Y. Tang, A. Koseska, J. Duan, and J. Kurths, Nat. Commun. **6**, 7709 (2015).
[30] G. Tanaka, K. Morino, and K. Aihara, in *Mathematical Approaches to Biological Systems*, edited by T. Ohira and T. Uzawa (Springer, New York, 2015), pp. 29–53.
[31] D. Gonze, S. Bernard, C. Waltermann, A. Kramer, and H. Herzel, Biophys. J. **89**, 120 (2005).
[32] J.-Y. Tinevez, F. Jülicher, and P. Martin, Biophys. J. **93**, 4053 (2007).
[33] K. Dierkes, B. Lindner, and F. Jülicher, Proc. Natl. Acad. Sci. U.S.A. **105**, 18669 (2008).
[34] J. Barral, K. Dierkes, B. Lindner, F. Jülicher, and P. Martin, Proc. Natl. Acad. Sci. U.S.A. **107**, 8079 (2010).
[35] R. M. Amro and A. B. Neiman, Phys. Rev. E **90**, 052704 (2014).
[36] J. Barral and P. Martin, Proc. Natl. Acad. Sci. U.S.A. **109**, E1344 (2012).
[37] F. Landis, T. Ott, and R. Stoop, Neural Comput. **22**, 273 (2010).
[38] G. E. Hinton and R. R. Salakhutdinov, Science **313**, 504 (2006).
[39] S. Bernard, D. Gonze, B. Čajavec, H. Herzel, and A. Kramer, PLoS Comput. Biol. **3**, e68 (2007).
[40] C. Bodenstein, M. Gosak, S. Schuster, M. Marhl, and M. Perc, PLoS Comput. Biol. **8**, e1002697 (2012).
[41] V. Šimonka, M. Fras, and M. Gosak, Physica A (Amsterdam) **424**, 1 (2015).
[42] G. K. Martin, B. L. Lonsbury-Martin, R. Probst, and A. C. Coats, Hear. Res. **33**, 49 (1988).
[43] C. L. Talmadge, G. R. Long, W. J. Murphy, and A. Tubis, Hear. Res. **71**, 170 (1993).
[44] E. Niebur, H. G. Schuster, and D. M. Kammen, Phys. Rev. Lett. **67**, 2753 (1991).
[45] B. Ananthasubramaniam, E. D. Herzog, and H. Herzel, PLoS Comput. Biol. **10**, e1003565 (2014).
[46] F. A. S. Ferrari, R. L. Viana, F. Gomez, T. Lorimer, and R. Stoop, New J. Phys. **17**, 055024 (2015).
[47] J. P. Keener, SIAM J. Appl. Math. **47**, 556 (1987).
[48] J. Schlesner, V. Zykov, H. Engel, and E. Schöll, Phys. Rev. E **74**, 046215 (2006).
[49] A. R. Champneys, V. Kirk, E. Knobloch, B. E. Oldeman, and J. Sneyd, SIAM J. Appl. Dyn. Syst. **6**, 663 (2007).
[50] D. Cumin and C. P. Unsworth, Physica D (Amsterdam) **226**, 181 (2007).
[51] M. Breakspear, S. Heitmann, and A. Daffertshofer, Front. Hum. Neurosci. **4**, 190 (2010).
[52] H. Hong and S. H. Strogatz, Phys. Rev. Lett. **106**, 054102 (2011).